Christos Karapanagiotis*, Marcus Schukar and Katerina Krebber

Distributed fiber optic sensors for structural health monitoring of composite pressure vessels

Verteilte faseroptische Sensoren zur Zustandsüberwachung von Verbundwerkstoff-Druckbehältern

https://doi.org/10.1515/teme-2023-0170
Received December 28, 2023; accepted January 31, 2024;
published online March 8, 2024

Abstract: In this paper, we present a comprehensive overview of our research in the field of distributed fiber optic sensors for structural health monitoring of hydrogen composite pressure vessels. Specifically, we demonstrate how the integration of fiber optic sensors into composite pressure vessels enhances safety while simultaneously reducing maintenance costs. The small size of optical fibers enables their integration into composite structures during the manufacturing process, allowing continuous monitoring and precise detection and localization of structural damages during service life. We also discuss the potential of state-of-the-art signal processing methods and machine learning for advancing predictive maintenance. Our applications of fiber optic sensors demonstrate their potential to contribute significantly to the energy transition towards renewable sources.

Keywords: distributed fiber optic sensors; composites; hydrogen pressure vessels; structural health monitoring; machine learning

Zusammenfassung: In diesem Beitrag geben wir einen umfassenden Überblick über unsere Forschung auf dem Gebiet der verteilten faseroptischen Sensorik für die strukturelle Zustandsüberwachung von Wasserstoffdruckbehältern aus Verbundwerkstoffen. Insbesondere zeigen wir, wie die Integration von faseroptischen Sensoren in Druckbehälter aus Verbundwerkstoffen die Sicherheit erhöht und gleichzeitig die Wartungskosten senkt. Die geringe Größe von Lichtwellenleitern ermöglicht ihre Integration in Verbundwerkstoffstrukturen während des Herstellungsprozesses, wodurch eine kontinuierliche Überwachung sowie eine präzise Erkennung und Lokalisierung von Strukturschäden während des Betriebs der Druckbehälter ermöglicht wird. Wir erörtern auch das Potenzial modernster Signalverarbeitungsmethoden und des maschinellen Lernens für die Weiterentwicklung der vorausschauenden Instandhaltung. Die von uns vorgestellten Anwendungen von faseroptischen Sensoren zeigen, dass sie einen wichtigen Beitrag zur Energiewende hin zu erneuerbaren Energien leisten können.

Stichworte: verteilte faseroptische Sensoren; Verbundwerkstoffe; Wasserstoff-Druckbehälter; Strukturüberwachung; maschinelles Lernen

1 Introduction

Composite materials have gained increasing attention across many sectors, including energy [1], [2]. Composites are made by reinforcing a polymer matrix with glass or carbon fibers and are characterized by a high strength-to-weight ratio, corrosion resistance, and low cost [3]. This opened the way for the fabrication of composite structures in the energy sector, including wind turbine blades, hydrogen pressure vessels, and pipelines [2], [4]–[6]. In the context of structural health monitoring (SHM), fiber optic sensors (FOS) offer unique solutions to safely prolong the lifespan of these composite structures and simultaneously reduce maintenance costs [7]–[10].

FOS posses a series of advantageous characteristics for SHM [11]. Specifically, they are immune to electromagnetic interference and allow operation in harsh environments. Of high importance for practical applications is the property of FOS to operate without reliance on external electricity or extensive cabling, minimizing the infrastructure required for measurements. FOS can be either pointwise or distributed sensors. While pointwise sensors, such as fiber Bragg gratings (FBG) measure only at specified positions [12], distributed fiber optic sensors (DFOS) acquire the spatial profiles of the fibers along tens of kilometers [13]–[16]. These profiles can be projected onto specific and complex geometries if desired. This eliminates the need for data

***Corresponding author: Christos Karapanagiotis**, Bundesanstalt für Materialforschung und -prüfung (BAM), Unter den Eichen 87, 12205 Berlin, Germany, E-mail: christos.karapanagiotis@bam.de.
https://orcid.org/0000-0002-9065-3480
Marcus Schukar, Bundesanstalt für Materialforschung und -prüfung (BAM), Berlin, Germany
Katerina Krebber, 8.6 Faseroptische Sensorik, Bundesanstalt fur Materialforschung und -prufung, Berlin, Germany

interpolation, a common requirement when dealing with point sensors. Additionally, the exceptional precision and accuracy of DFOS enable the precise localization of signal features and anomalies across the entire sensing length [17], [18]. DFOS necessitate either one or two access points and can be conveniently accommodated within tight spaces due to their small size.

FOS have been widely applied in the field of SHM [19], [20]. In civil engineering, FOS provide condition monitoring of bridges, tunnels and buildings, contributing to the structure's stability and longevity [21]–[23]. Additionally, FOS have proven valuable in geotechnical engineering, enhancing the safety and efficiency of structures such as dams by monitoring stress distribution and deformation [24]. Furthermore, FOS have been employed for monitoring transportation networks, including railways and roads [25]–[28]. Beyond these areas, FOS demonstrate its effectiveness in the oil and gas industry for condition monitoring of long pipelines [29]. Even in renewable and green energy sectors, FOS made an impact by assessing structural integrity and enhancing safety measures of wind turbines [30]–[32], subsea cables [33], [34], and hydrogen pressure vessels [9], [10].

FOS, as a well-established SHM technique, has also been applied in the field of composites [35]–[39]. Optical fibers, due to their small size, can be embedded in composites and used as sensing elements to measure a wide range of parameters including temperature, humidity, strain, and vibrations [40]–[47]. In addition, FOS have been used to detect structural deformations caused mainly by delamination or cracks after fatigue tests [48]–[51], and impact damages [52], [53].

Hydrogen is usually stored in vessels under very high pressure [54], and thus DFOS can be used to ensure structural integrity of composite pressure vessels. These vessels are fabricated with a substantial safety margin to eliminate any potential risk. Moreover, to guarantee safety, they also undergo periodic inspections throughout their designated service life [55]. SHM, on the other hand, can significantly reduce maintenance costs, allow longer service life, and increase safety by providing continuous condition monitoring. The integration of optical fibers in the composite structure and use of distributed sensing techniques, such as optical frequency domain reflectometry (OFDR) [56], allows monitoring in all positions that the fiber is placed, which can be very useful to locate changes of the vessel's structural behavior [9], [57]–[59].

In this paper, we provide a comprehensive overview of our research in the field of DFOS for SHM of composite pressure vessels and make a connection between conventional and modern machine learning methods towards predictive maintenance. Specifically, the paper is structured as follows: In the second chapter, we provide an overview of the most known DFOS technologies focusing on OFDR. In the third chapter, we provide examples of DFOS applications on composite pressure vessels. In the fourth chapter, we discuss new opportunities that arise with the emergence of machine learning in the context of advanced signal processing and predictive maintenance.

2 Distributed fiber optic sensors

Unlike pointwise sensors that measure only at specified positions, DFOS measure continuously along the entire length of an optical fiber [11]. DFOS are primarily categorized based on their scattering mechanisms, which involve Rayleigh, Brillouin, or Raman effects [11], as shown in Figure 1. Rayleigh-based DFOS operate by detecting the backscattered light resulting from interactions with the fiber's inherent refractive index fluctuations. This approach yields the strongest signal and, thus, it does not necessitate signal averaging. This renders Rayleigh-based DFOS well-suited for dynamic sensing applications [60]. It is worth noting that Rayleigh-based DFOS systems, operating in either the time or frequency domain, have been developed [61]. On the other hand, Brillouin-based DFOS rely on detecting Brillouin scattering resulting from the interaction between light and acoustic waves propagating within the fiber. This technique is very robust and provides measurements of temperature and strain over km-long distances [13]–[16]. However, Brillouin scattering is relatively weaker compared to Rayleigh scattering, often requiring signal averaging to

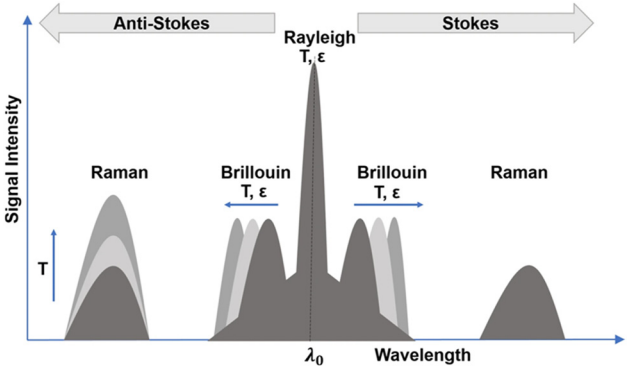

Figure 1: Schematic representation of Rayleigh, Brillouin, and Raman scattering effects in optical fibers providing a rough estimation of the backscattered intensity or frequency changes with temperature or strain. Copyright 2021, licensed under a Creative Commons Attribution 4.0 International license [7].

achieve a high signal-to-noise ratio (SNR). Consequently, Brillouin-based DFOS are better suited for static or quasi-static monitoring applications where changes occur over extended periods. Nonetheless, it is noteworthy that solutions for dynamic Brillouin DFOS have also been proposed [62]–[64].

In this paper, we use a distributed fiber optic sensing technology based on swept wavelength interferometry and specifically the commercial device LUNA OBR (Luna Innovations, Inc., USA). The technology requires access to one end of the fiber and is based on Rayleigh scattering which arises from the light traveling down the fiber and inhomogeneities in the material. LUNA OBR represents a polarization-diverse adaptation of optical frequency domain reflectometry (OFDR), which according to the manufacturer enhances sensitivity and resolution [65]. A schematic representation of the basic system is shown in Figure 2a. The system consists of a tunable laser source (TLS) that sweeps frequencies in a wavelength range of $\Delta\nu$ around a center wavelength of 1550 nm. The light is split into the reference and measurement paths of the interferometer. The measurement path contains the sensing fiber (fiber-under-test (FUT)). With the help of a polarization controller (PC) and a polarization beam splitter (PBS), the interference of the measurement field with two perpendicular polarization states is obtained at S and P detectors. The complex reflection coefficients that are obtained from the two detectors after a frequency sweep are converted into the time domain using inverse fast Fourier transformations (iFFT). Using the fiber's refractive index, the time domain trace can be represented as a function of length.

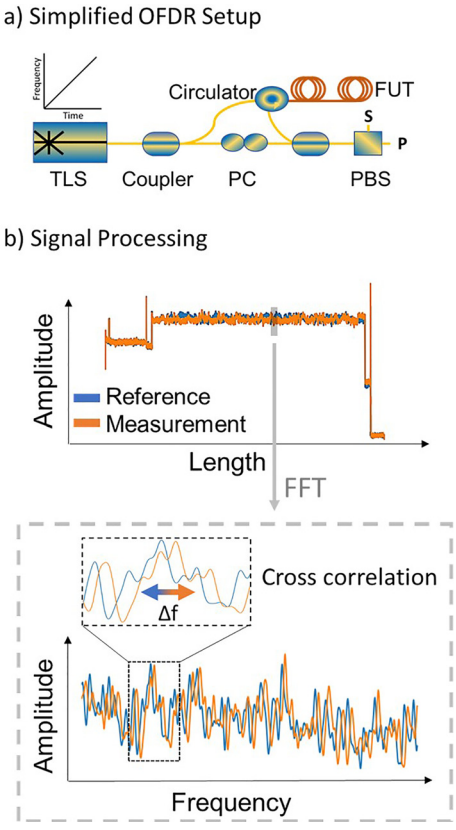

Figure 2: OFDR setup and signal processing. (a) Simplified representation of an optical frequency domain reflectometry (OFDR) system. (b) Schematic representation of the system's signal processing. The backscatter profiles (top) of the measurement and the reference signals are divided into segments defined by the gauge length. Each segment (grey frame) is transformed into a frequency domain via fast Fourier transformations (FFT) and the frequency shift between reference and measurement signal is calculated using cross-correlation (bottom).

This technique measures temperature or strain changes, and thus the recording of a reference measurement is necessary. As an example, Figure 2b shows two traces, one in blue representing the reference and another in orange representing the measurement. To analyze these traces and extract spatially resolved temperature or strain changes, it is necessary to divide the traces into segments. These segments' lengths are defined by the so-called "gauge length", which determines the desired spatial resolution. The segments are then transformed back to the frequency domain using fast Fourier transformations (FFT) as shown in Figure 2b. The spectral shift (Δf) of each segment is estimated by cross-correlation. Cross-correlation quantifies the similarity between two signals by sliding one over the other and computing the measure of similarity at each position as follows:

$$z[k] = (R * M)(k - \|R\|) \tag{1}$$

where R is the reference signal, M is the measurement signal, $\|R\|$ is the length of the reference signal, and $k = 0, 1, \ldots, 2\|R\| - 2$. After the correlation function $z[k]$ is obtained, the spectral shift can be extracted by the position of the maximum value as follows:

$$\delta\nu = \frac{\Delta\nu}{\|R\|}\left(\underset{k}{argmax}\big(z[k]\big) - \|R\| + 1\right) \tag{2}$$

The spectral shift is linearly related to temperature and strain changes with coefficients depending on the fiber's refractive index [56].

3 Monitoring of composite pressure vessels

In the past years and before monitoring composite pressure vessels, we have applied DFOS to measure strain and

structural deformations of simpler composite structures such as glass fiber-reinforced polymer (GFRP) tubes. These results, as published in [51], [66], [67], showed that DFOS and scanning wavelength interferometry-based sensing techniques, in particular, are promising for structural health monitoring applications. Specifically, we demonstrated that DFOS can detect structural damages at an early stage by providing strain information along the entire length of the optical fiber with spatial resolution down to the millimeter range. In this section, however, we will provide an overview of our DFOS applications on composite pressure vessels designed for hydrogen storage.

The type of optical fibers is of high importance in DFOS. In Figure 3 we show a comparison of the backscattered amplitude of an acrylate-coated SMF28e+ (Corning Inc.) optical fiber and a polyimide (PI)-coated SM1500(4.2/80)PI (Fibercore Ltd) optical fiber. As we observe, the PI-coated optical fiber has a backscattered amplitude of approximately 10 dB higher than that of the acrylate-coated optical fiber, which in practice results in higher strain accuracy. The higher backscattered amplitude is attributed to the fiber's enhanced germanium doping and higher numerical aperture [68]. Based on these results, for monitoring composite pressure vessels, we made use of the SM1500(4.2/80)PI.

The composite pressure vessels are categorized mainly into five types, as shown in Table 1. In this paper, we demonstrate DFOS applied only in composite vessels of type III and IV. The difference between type III and IV is that the first is made by a metal liner while the second, by a plastic liner [54]. The plastic liner is lighter which makes type IV vessels attractive for a series of applications, including the automobile industry. For the sake of completeness, we mention that the older types, namely type I and type II, are significantly heavier, withstand lower pressure levels, and have lower storage capacity [1], [54]. The newest vessels of type V do not have an internal liner and could result in increased fatigue performance [1].

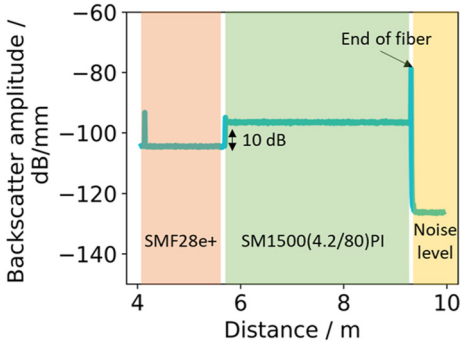

Figure 3: Comparative analysis of backscatter amplitudes between a standard acrylate-coated optical fiber (SMF28e+) and a polyimide-coated optical fiber with enhanced doping and high numerical aperture (SM1500(4.2/80)PI).

Table 1: An overview of composite pressure vessel types.

Type	Materials	Liner	Typical pressure
Type I	Metal	N/A	<300 bar
Type II	Mostly metal with hoop-wrapped composites	Metal	<300 bar
Type III	Fully-wrapped composites	Metal	<700 bar
Type IV	Fully-wrapped composites	Polymer	<700 bar
Type V	Fully-wrapped composites	N/A	<700 bar

The structural body of an overwrapped composite pressure vessel is typically manufactured by a process called filament winding [57]. This involves the wrapping of carbon or glass fibers under tension around the vessel's liner at specified angles. The thickness of the composite layer as well as the whole winding process is strongly related to the vessel's bearing capacity [69]. During the winding process, segments of optical fibers can also be integrated into the composite layer. We note that the wrapping of the optical fiber is performed in the same way as the composite fibers. However, for sensing purposes, at least one end of the optical fiber must be accessible when the filament winding is finished. Figure 4 shows the filament winding procedure where glass fibers cover an optical fiber encased in a yellow protective jacket. As we have shown in [9], when the pitch angle of the carbon or glass fibers and the optical fibers are nearly identical, then resin pockets and voids surrounding the optical fiber are negligible. For the sake of completeness, we note that resin pockets are areas with an excess of resin used to bind composite materials, while voids are empty spaces that can weaken the material's structural integrity when not properly filled during manufacturing [70].

Apart from integrating the optical fiber into the composite structure, one can also affix it to the surface of a

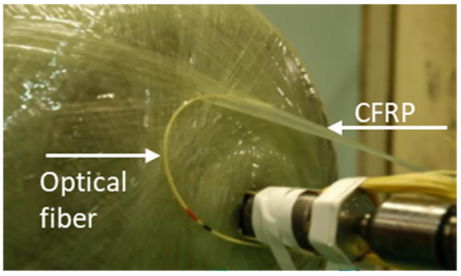

Figure 4: Filament winding of glass fiber reinforced polymers (GFRP) covering an optical fiber encased in a yellow protective jacket. The vessel has a total length and diameter of 80 cm and a 30 cm, respectively.

vessel [58]. This alternative method has some positive aspects, including simplified configuration and cost efficiency, as it eliminates the need for specialized equipment required for fiber integration. Furthermore, when the optical fibers are integrated and placed in close proximity to the liner, this could pose a risk to the integrity of the fiber due to potential composite structural deformations during operation. However, we need to mention that integrating optical fibers into the composite structure provides protection to the fibers from potential damage caused by external factors.

Figure 5 shows an example of surface-applied optical fibers on a type III composite vessel. This vessel is made with an aluminum liner, carbon fiber-reinforced polymers (CFRP), and outer layers of glass fiber-reinforced polymers (GFRP). Furthermore, the outer surface is also covered by sealing, primer, and lacquer. The optical fibers are attached in a radial and axial direction on the grey zones where the outer layers up to the GFRP are removed. We note that these layers are removed because tests have shown that lacquer affects the measured strain caused by local surface damages.

The direction of the optical fibers affects significantly the pressure sensitivity. Figure 6a and b shows the strain profiles at three different pressure levels that correspond to the optical fiber segments applied in the axial (a) and radial direction (b). The strain fluctuations observed in these plots are related to the vessel's local mechanical properties. Figure 6c shows that strain measured in both directions increases linearly with pressure. However, the pressure sensitivity measured in µm/m/bar in the radial direction is approximately 1.8 times higher than that in the axial direction. This renders the wrapping of the optical fibers in the radial direction more favorable for monitoring.

Figure 7a shows the strain profile along the optical fiber when the vessel is pressurized. The optical fiber is integrated into the composite structure and close to the outer surface, in particular. The optical fiber passes through the dome area with the connection port (depicted in the yellow frame), the cylindrical area, and the blind dome area (depicted in the green frame) several times. For the sake of clarity, in Figure 7c we provide a schematic representation of the position of the optical fiber in the dome area where the connection port is located. We note that the strain profiles can be correlated with positions on the vessel's surface based on the parameters established during the winding of the optical fiber. These parameters include the ingress and egress positions, the length of the optical fiber, and the winding angle. As can be seen, the optical fiber passes three times from that dome area, which corresponds to the number of yellow frames in the plots above. In Figure 7a it can be observed that, under constant pressure, the measured strain is higher in the dome areas than in the cylindrical section. This can be attributed to the thickness of the composite material and the optical fiber configuration that differs from the cylindrical part to the dome areas.

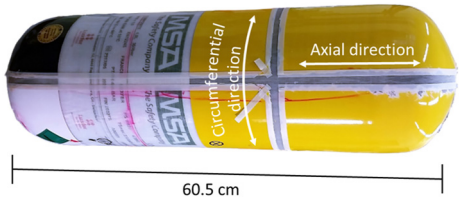

Figure 5: Optical fibers applied on the surface of a type III composite overwrapped pressure vessel. The vessel has a total length and diameter of 60.5 cm and a 15 cm, respectively.

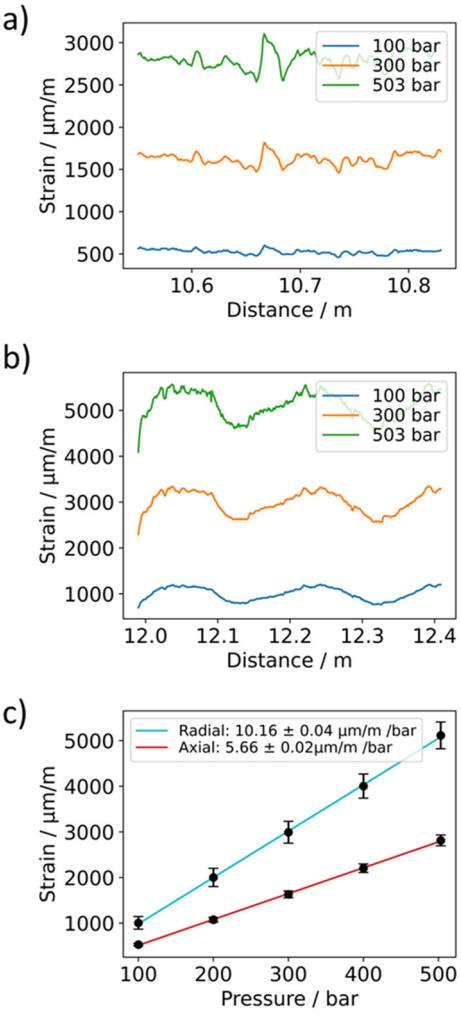

Figure 6: Distributed strain profiles corresponding to the optical fiber segments applied to the axial (a) and radial (b) direction of the pressure vessel. (c) Comparison of the pressure sensitivity of the two optical fiber segments. The dots correspond to the mean values of the two segments as shown in (a) and (b), while the error bars to the standard deviation.

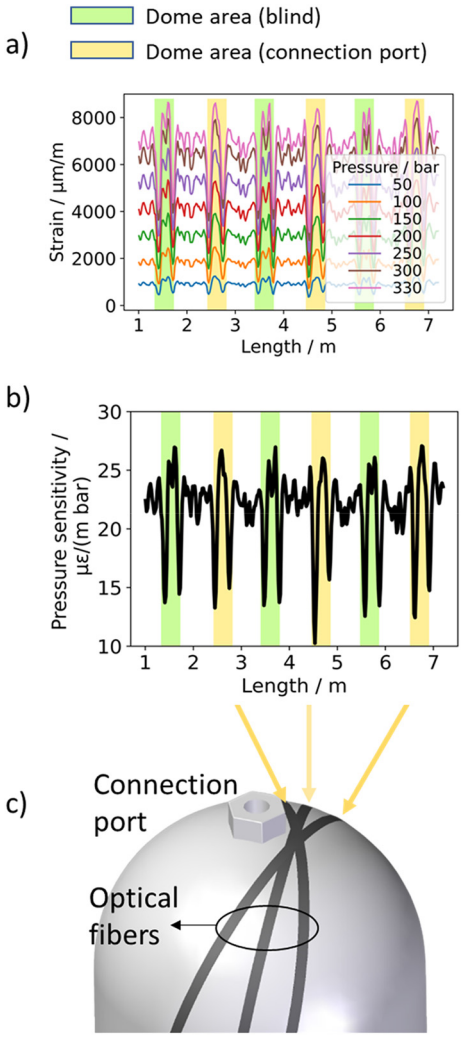

Figure 7: Pressure-dependent strain profile and sensitivity analysis of the integrated optical fiber. (a) Strain profile along the length of the optical fiber measured at different pressure levels from 50 bar to 330 bar. The green and yellow frames indicate the sensing positions at the blind dome area and at the dome area with the connection port, respectively. The areas without a colored background correspond to the cylindrical part of the vessel. (b) Pressure sensitivity along the length of the optical fiber. (c) Schematic representation of the position of the integrated optical fiber in the dome area with the connection port.

Furthermore, as expected, the strain increases linearly with pressure, with the pressure sensitivity depending on the position of the fiber. Figure 7b shows the pressure sensitivity along the entire length of the fiber extracted by linear fitting. As can be seen, the pressure sensitivity in the cylindrical part and the dome areas is approximately 22 µm/m/bar and 25 µm/m/bar, respectively.

Figure 7 shows not only the variation in strain and pressure sensitivity between the cylindrical section and the dome areas but also strain variations within the dome areas themselves. As we have already shown in Figure 6, the measured strain depends, apart from the composite material thickness, on the wrapping angle of the optical and the carbon fibers, respectively. Therefore, the strain fluctuations observed within the dome areas are attributed to the complex geometry and varying wrapping angles in these specific regions. Furthermore, as can be seen in Figure 7b, not only the strain but also the pressure sensitivity depends on the orientation of the embedded optical fibers.

DFOS allow damage detection and localization. Figure 8a shows a vessel that burst after approximately 250,000 pressure cycles from 0 bar to 330 bar. As can be seen, the damage occurred in the dome area with the connection port, which was completely ejected after the burst. In Figure 8b, we trace the damage progress during the last load pressure cycles before bursting for the same fiber that we used before. We note that the strain profiles were acquired under constant pressure and specifically at 330 bar. We observe three distinct sections with increasing strain changes along the length of the sensing fiber. These sections correspond to the dome area with the connection port. This indicates that the location of the failure is in that dome area. The highest strain changes in the middle of the sensing fiber indicate that the fiber segment at 4.6 m is closer to the damage. The other two peaks exhibit

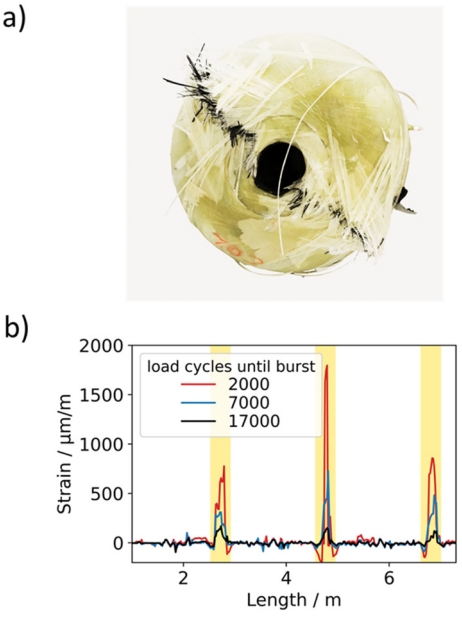

Figure 8: Pressure vessel and strain profile after burst. (a) Composite pressure vessel after burst with the connection port totally ejected. (b) Strain profile along the optical fiber measured at 330 bar and different load cycles before burst. The yellow frames indicate the positions that correspond to the dome with the connection port.

comparatively lower strain changes, indicating a larger distance from the damage.

These results demonstrate the potential of predictive maintenance and estimation of the remaining operational lifetime of pressure vessels with fiber optic sensors. As can be seen, signs of damage occurred many load cycles before the failure, which could give a signal that the vessel is not safe to operate any longer.

When applying FOS, temperature and strain cross-sensitivity is of high importance. In practice, an accurate estimation of strain changes between two measurements requires an environment of constant temperature. However, in cases where temperature change is present, temperature compensation can be applied assuming that the temperature change, the fiber's temperature sensitivity, and the vessel's thermal expansion coefficient are known. The fiber's temperature sensitivity is sometimes provided by the manufacturer but, in any case, it can be easily estimated by exposing a fiber segment at specified temperature conditions. On the other hand, the vessel's thermal expansion coefficient is not the same on the whole surface and, thus, the vessel with the integrated fibers needs also to be exposed at specified temperature levels before the load cycles, so that the thermal expansion coefficient at every position can be estimated.

4 Towards machine learning-based monitoring

In the past few years, machine learning has revealed new capabilities in advanced signal processing creating opportunities for innovation and progress in the field of fiber optic sensors [71]–[73]. In previous papers, we presented an artificial neural network (ANN)-based approach for replacing cross-correlation in wavelength-scanning coherent optical time-domain reflectometry (WS-COTDR) [74]. As reported, ANNs increase strain accuracy when the SNR is low and reduce signal processing time considerably. We believe that this machine learning solution could also have a positive impact on OFDR signal processing.

Figure 9a shows a reference and a measurement signal in the frequency domain, whose spectral shift is not clear as in Figure 2b. In these cases of low SNR, the employment of the standard cross-correlation often results in erroneous estimations of spectral shifts. ANNs can be very tolerant to noise and focus on essential patterns in the signals, which in this particular case could lead to more precise spectral shift estimations. The network's structure and the hyperparameters can be optimized after a systematic study of their

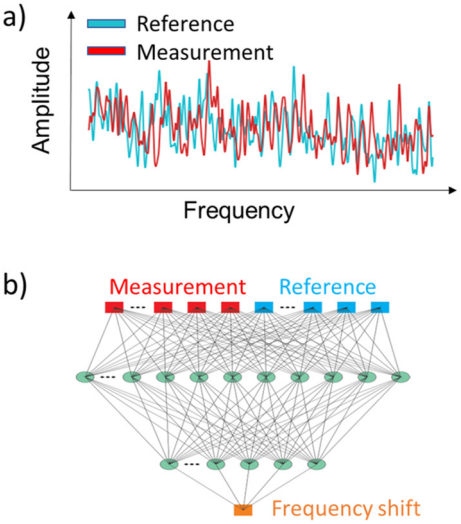

Figure 9: (a) LUNA OBR reference (blue) and measurement signal (red) in the frequency domain, where the frequency shift is not visible. (b) An artificial neural network (ANN) architecture for estimation of the spectral shift from the two signals.

impact on the model's performance. The proposed ANN architecture is shown in Figure 9b. It consists of an input layer containing the reference and measurement signals in the frequency domain, two hidden layers, and a single output layer responsible for determining the frequency shift. We note that this architecture is similar to the one used in [74]. For training such an ANN one could use synthetic data, while for the performance evaluation, real experimental data should be collected. Assuming that the application of this machine learning approach will bring similar benefits in strain calculation to those reported in [74], our methods are expected to become even more attractive in the field of SHM.

In [66] we showed that a set high spatial resolution affects negatively the performance of the cross-correlation which in turn results in strain outliers. This is attributed to the fact that the number of points in the signal segments used for the cross-correlation calculation reduces when the spatial resolution increases. In [74] we showed that ANN-based cross-correlation can deal very well with sparse signals, and thus we believe that the spatial resolution could also benefit from an ANN-based approach as already described.

Machine learning could also be used to facilitate the monitoring of more than one parameter [72], [75]. As we have discussed in the last paragraph of the third section, in case of temperature changes, the temperature effects need to be compensated to extract accurate strain information. Methods to address the cross-sensitivity include the use of two optical fibers, the use of a polarization-maintaining

fiber, or even the exploitation of more than one scattering effect [76]–[80]. Many studies have shown that when machine learning is combined with these solutions, the performance in terms of temperature and strain accuracy can be enhanced significantly [18], [72].

Apart from improving strain and temperature accuracy, machine learning can be used to analyze the extracted strain profiles and detect signs of damages. Although high strain values can indicate potential damages, as shown in Figure 8b, signs of damages are not always easy to be identified with conventional methods. For this reason, machine learning methods have been widely employed in the field of SHM to detect damages even at an early stage [71], [81], [82]. However, the training of machine learning models requires feature extraction from the data. Apart from the strain change over time, as shown in Figure 8b, one could also make use of the pressure sensitivity as presented in Figure 7b. Over the course of load cycles, not only the strain but also the pressure sensitivity changes at the positions that correspond to the blind dome area. Figure 10 illustrates the variation of strain with pressure at a constant location (4.7 m) in the dome area with the connection port. The observed data correspond to measurements taken during distinct load pressure cycles, specifically at 22,000, 17,000, 7000, and 2000 load cycles before the vessel's burst. Furthermore, the strain also starts deviating from a perfect linear relationship with pressure. This could indicate that the pressure sensitivity as well as its error could be informative features for predicting failures. A quantitative analysis of these values is shown in Table 2.

In order to train reliable machine learning models for damage prediction and even predictive maintenance, more experiments are required. In the future, we plan to train models based on a plethora of data collected from similar experiments. A larger dataset will also allow more features to be extracted similar to those used for SHM based on other types of sensors. These features could be statistical parameters (maximum, minimum value, and mean value, skewness, kurtosis, variance) [83], [84], parameters of time-fitted data (autocorrelation coefficients) [85] or even time-frequency domain properties (Wigner-Ville transform, Discrete Fourier/Wavelet transform) [86], [87]. Such features could also be extracted from FOS data to facilitate the detection of anomalies that indicate damages [83].

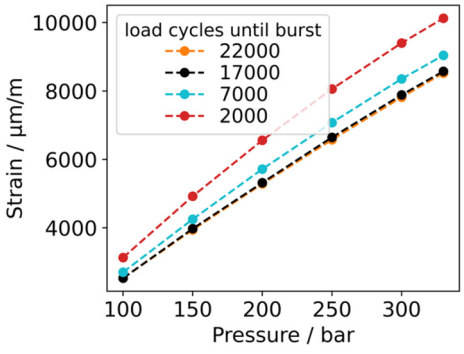

Figure 10: Evolution of strain at a fixed position resulted from measurements conducted at different load cycles prior to the burst event.

Table 2: Pressure sensitivity and its error resulted from measurements conducted at different load cycles prior to the burst event.

Cycles before burst	Pressure sensitivity µm/m/bar	Error of pressure sensitivity µm/m/bar
22,000	26.03	0.38
17,000	26.27	0.44
5000	27.55	0.64
2000	30.34	0.97

The interpretability of the model in predictive maintenance is of high importance and depends strongly on the machine learning algorithm [88]. Complex machine learning models such as ANNs or convolutional neural networks (CNNs) are very powerful and often do not require manual feature extraction, but this comes at the cost of difficult interpretation of the results. For this reason, we believe that a methodology based on feature extraction as described previously and simpler models such as decision trees, k-nearest neighbor regression, ridge regression, or even simple linear and polynomial regression could be advantageous. In order to further facilitate interpretability and build a model that delivers not only a single output but also a probability distribution, we will employ models such as Bayesian statistics, as we have recently done in [89]. The model can be either a classifier or a regressor. The output of the classifier can be either "safe" or "risk" to indicate a safe operation or the need for inspection or replacement, respectively. On the other hand, a regression model could output the remaining operational lifetime.

5 Conclusions

We presented an overview of our research in applied distributed fiber optic sensors (DFOS) for structural health monitoring of composite pressure vessels. We showed that optical fibers can be successfully embedded into composite pressure vessels during their manufacturing process with the optical fiber's winding angle affecting the vessel's monitoring considerably. DFOS demonstrated the ability to identify and localize structural deformations even at the vessel's dome areas. Furthermore, we proposed machine learning

methods based on artificial neural networks and other algorithms to advance signal processing and allow predictive maintenance. We believe that DFOS can positively impact the energy transition by enhancing safety, reducing maintenance costs, and prolonging operational lifetimes of composite structures used in the energy sector such as hydrogen pressure vessels and wind turbine blades.

Acknowledgments: The authors would like to thank their partners from the research project COD-AGE for the great collaboration. We would also like to thank our colleagues and partners within the QI-Digital initiative and especially the head of the pilot project "Reliable hydrogen refueling stations" Georg Mair. Special thanks to our colleague at BAM Eric Duffner for his support.

Research ethics: Not applicable.

Author contributions: The authors have accepted responsibility for the entire content of this manuscript and approved its submission.

Competing interests: The authors state no competing interests.

Research funding: German Ministry of Economic Affairs and Climate Actions.

Data availability: The raw data can be obtained on request from the corresponding author.

References

[1] A. Air, M. Shamsuddoha, and B. Gangadhara Prusty, "A review of Type V composite pressure vessels and automated fibre placement based manufacturing," *Composites, Part B*, vol. 253, p. 110573, 2023.

[2] L. Mishnaevsky, K. Branner, H. Petersen, J. Beauson, M. McGugan, and B. Sørensen, "Materials for wind turbine blades: an overview," *Materials*, vol. 10, no. 11, p. 1285, 2017.

[3] S. Hegde, B. Satish Shenoy, and K. N. Chethan, "Review on carbon fiber reinforced polymer (CFRP) and their mechanical performance," *Mater. Today: Proc.*, vol. 19, no. 2, pp. 658—662, 2019.

[4] F. G. Alabtah, E. Mahdi, and F. F. Eliyan, "The use of fiber reinforced polymeric composites in pipelines: a review," *Compos. Struct.*, vol. 276, p. 114595, 2021.

[5] M. Azeem, *et al*., "Application of filament winding technology in composite pressure vessels and challenges: a review," *J. Energy Storage*, vol. 49, p. 103468, 2022.

[6] C. P. Fowler, A. C. Orifici, and C. H. Wang, "A review of toroidal composite pressure vessel optimisation and damage tolerant design for high pressure gaseous fuel storage," *Int. J. Hydrogen Energy*, vol. 41, no. 47, pp. 22067—22089, 2016.

[7] M. Ramakrishnan, G. Rajan, Y. Semenova, and G. Farrell, "Overview of fiber optic sensor technologies for strain/temperature sensing Applications in composite materials," *Sensors*, vol. 16, no. 1, p. 99, 2016.

[8] R. O. Claus, *et al*., "Fiber optic impact detection and location system embedded in a composite material," in *In the Proceedings of Fiber Optic Smart Structures and Skins V*, Boston, USA, 1992, pp. 262—269.

[9] D. Munzke, *et al*., "Monitoring of type IV composite pressure vessels with multilayer fully integrated optical fiber based distributed strain sensing," *Mater. Today: Proc.*, vol. 34, no. 1, pp. 217—223, 2021.

[10] G. Souza and J. R. Tarpani, "Using OBR for pressure monitoring and BVID detection in type IV composite overwrapped pressure vessels," *J. Compos. Mater.*, vol. 55, no. 3, pp. 423—436, 2020.

[11] A. H. Hartog, *An Introduction to Distributed Optical Fibre Sensors*, Boca Raton, FL, USA, CRC Press, Taylor & Francis Group, 2017.

[12] K. O. Hill and G. Meltz, "Fiber Bragg grating technology fundamentals and overview," *J. Lightwave Technol.*, vol. 15, no. 8, pp. 1263—1276, 1997.

[13] T. Kapa, A. Schreier, and K. A. Krebber, "100-km BOFDA assisted by first-order bi-directional Raman amplification," *Sensors*, vol. 19, no. 7, p. 1527, 2019.

[14] X. Sun, *et al*., "Ultra-long Brillouin optical time-domain analyzer based on distortion compensating pulse and hybrid lumped—distributed amplification," *APL Photonics*, vol. 7, p. 126107, 2022.

[15] M. A. Soto, G. Bolognini, and F. Di Pasquale, "Optimization of long-range BOTDA sensors with high resolution using first-order bi-directional Raman amplification," *Opt. Express*, vol. 19, no. 5, pp. 4444—4457, 2011.

[16] Z. Yang, X. Sun, X. Hong, S. Jin, M. A. Soto, and J. Wu, "400 km-loop BOTDA enabled by hybrid amplification based on distributed Raman and Erbium-doped fibers," in *In the Proceedings of 27th International Conference on Optical Fiber Sensors*, Alexandria, USA, 2002, p. F2.1.

[17] H. C. H. Li, I. Herszberg, C. E. Davis, A. P. Mouritz, and S. C. Galea, "Health monitoring of marine composite structural joints using fibre optic sensors," *Compos. Struct.*, vol. 75, no. 4, pp. 321—327, 2006.

[18] A. Venketeswaran, *et al*., "Recent advances in machine learning for fiber optic sensor applications," *Adv. Intell. Syst.*, vol. 4, no. 1, p. 2100067, 2021.

[19] M. F. Bado and J. R. Casas, "A review of recent distributed optical fiber sensors applications for civil engineering structural health monitoring," *Sensors*, vol. 21, no. 5, p. 1818, 2021.

[20] B. G. Gorshkov, *et al*., "Scientific applications of distributed acoustic sensing: state-of-the-art review and perspective," *Sensors*, vol. 22, no. 3, p. 1033, 2022.

[21] A. Minardo, R. Bernini, L. Amato, and L. Zeni, "Bridge monitoring using Brillouin fiber-optic sensors," *IEEE Sens. J.*, vol. 12, no. 1, pp. 145—150, 2012.

[22] A. Minardo, *et al*., "Long-term monitoring of a tunnel in a landslide prone area by Brillouin-based distributed optical fiber sensors," *Sensors*, vol. 21, no. 21, p. 7032, 2021.

[23] C. M. Monsberger, P. Bauer, F. Buchmayer, and W. Lienhart, "Large-scale distributed fiber optic sensing network for short and long-term integrity monitoring of tunnel linings," *J. Civ. Struct. Health*, vol. 12, pp. 1317—1327, 2022.

[24] L. Zeni, *et al*., "Brillouin optical time-domain analysis for geotechnical monitoring," *J. Rock Mech. Geotech. Eng.*, vol. 7, no. 4, pp. 458—462, 2015.

[25] G. Cedilnik, R. Hunt, and G. Lees, "Advances in train and rail monitoring with DAS," in *Proceedings of 26th International*

Conference on Optical Fiber Sensors, Lausanne, Switzerland, 2018, p. ThE35.

[26] S. Kowarik, *et al*., "Fiber optic train monitoring with distributed acoustic sensing: conventional and neural network data analysis," *Sensors*, vol. 20, no. 2, p. 450, 2020.

[27] D. Milne, A. Masoudi, E. Ferro, G. Watson, and L. Le Pen, "An analysis of railway track behaviour based on distributed optical fibre acoustic sensing," *Mech. Syst. Signal Process.*, vol. 142, p. 106769, 2020.

[28] K. Hicke, S. Chruscicki, and S. Münzenberger, "Urban traffic monitoring using distributed acoustic sensing along laid fiber optic cables," in *In the Proceedings of EAGE GeoTech 2021 Second EAGE Workshop on Distributed Fibre Optic Sensing, Online Event*, 2021, pp. 1—3.

[29] X. Lu, M. Schukar, S. Großwig, U. Weber, and K. Krebber, "Monitoring acoustic events in boreholes using wavelength-scanning coherent optical time domain reflectometry in multimode fiber," in *In the Proceedings of EAGE GeoTech 2021 Second EAGE Workshop on Distributed Fibre Optic Sensing; Online Event*, 2021, pp. 1—5.

[30] K. Krebber, W. Habel, T. Gutmann, and C. Schram, "Fiber Bragg grating sensors for monitoring of wind turbine blades," in *In the Proceedings of 17th International Conference on Optical Fibre Sensors*, Belgium, Bruges, 2005, p. 5855.

[31] A. Coscetta, *et al*., "Wind turbine blade monitoring with Brillouin-based fiber-optic sensors," *J. Sens.*, vol. 2017, pp. 1—5, 2017.

[32] K. Krebber, W. Habel, T. Gutmann, and C. Schramm, "Monitoring of the rotor blades of wind turbines by fibre optic sensors," in *In the Proceedings of the 3rd International Conference on Materials Testing*, Nürnberg, TEST, 2005, pp. B.5-55—B.55-60.

[33] A. Masoudi, J. A. Pilgrim, T. P. Newson, and G. Brambilla, "Subsea cable condition monitoring with distributed optical fiber vibration sensor," *J. Lightwave Technol.*, vol. 37, no. 4, pp. 1352—1358, 2019.

[34] M. A. Graf, F. Ehmer, C. Eisermann, M. Jakobi, and A. W. Koch, "Faseroptische Überwachung von mechanisch deformierten Kabelgeflechtsstrukturen mittels optischer Zeitbereichsreflektrometrie/Fiber-optic monitoring of mechanically deformed cable structures by means of optical time-domain reflectometry," *Tech. Mess.*, vol. 85, no. s1, pp. 73—79, 2018.

[35] G. Rajan and B. G. Prusty, *Structural Health Monitoring of Composite Structures Using Fiber Optic Methods*, Boca Raton, FL, USA, CRC Press, 2016.

[36] R. Di Sante, "Fibre optic sensors for structural health monitoring of aircraft composite structures: recent advances and applications," *Sensors*, vol. 15, no. 8, pp. 18666—18713, 2015.

[37] A. Güemes, A. Fernández-López, P. Díaz-Maroto, A. Lozano, and J. Sierra-Perez, "Structural health monitoring in composite structures by fiber-optic sensors," *Sensors*, vol. 18, no. 4, p. 1094, 2018.

[38] I. García, J. Zubia, G. Durana, G. Aldabaldetreku, M. Illarramendi, and J. Villatoro, "Optical fiber sensors for aircraft structural health monitoring," *Sensors*, vol. 15, no. 7, pp. 15494—15519, 2015.

[39] L. S. M. Alwis, K. Bremer, F. Weigand, M. Kuhne, R. Helbig, and B. Roth, "Evaluation of the potential of fiber optic sensors for structural health monitoring of carbon fiber-reinforced concrete composites," in *In the Proceedings of Optical Fiber Sensors Conference 2020 Special Edition*, Washington DC, USA, 2020, p. W4.66.

[40] C. V. O'Keefe, B. B. Djordjevic, and B. N. Ranganathan, "Multi-Parameter Fiber optic sensing for composite material monitoring," in *In the Proceedings of Nondestructive Characterization of Materials VI*, Boston, USA, 1994, pp. 363—368.

[41] C. Doyle, *et al*., "In-situprocess and condition monitoring of advanced fibre-reinforced composite materials using optical fibre sensors," *Smart Mater. Struct.*, vol. 7, pp. 145—158, 1998.

[42] A. K. Green, M. Zaidman, E. Shafir, M. Tur, and S. Gali, "Infrastructure development for incorporating fibre-optic sensors in composite materials," *Smart Mater. Struct.*, vol. 9, pp. 316—321, 2000.

[43] J. Montesano, M. Selezneva, C. Poon, Z. Fawaz, and K. Behdinan, "Application of fiber optic sensors for elevated temperature testing of polymer matrix composite materials," *Sci. Eng. Compos. Mater.*, vol. 18, no. 1—2, pp. 109—116, 2011.

[44] C. Miguel Giraldo, J. Zúñiga Sagredo, J. Sánchez Gómez, and P. Corredera, "Demonstration and methodology of structural monitoring of stringer runs out composite areas by embedded optical fiber sensors and connectors integrated during production in a composite plant," *Sensors*, vol. 17, no. 7, p. 1683, 2017.

[45] C. Sonnenfeld, *et al*., "Microstructured optical fiber sensors embedded in a laminate composite for smart material applications," *Sensors*, vol. 11, no. 3, pp. 2566—2579, 2011.

[46] J. M. López-Higuera, *et al*., "Evaluating distributed fibre optic sensors integrated into thermoplastic composites for structural health monitoring," in *In the Proceedings of 23rd International Conference on Optical Fibre Sensors*, Santander, Spain, 2014, p. 91575Q.

[47] R. d. Oliveira, M. Schukar, K. Krebber, and V. Michaud, "Distributed strain measurement in CFRP structures by embedded optical fibres: influence of the coating," in *In the Proceedings of the 16th International Conference on Composite Structures*, Porto, Portugal, 2011.

[48] M. Frovel, *et al*., "Robust integration of optical fiber sensors for aerospace applications in composite material structures," in *In the Proceedings of the 8th European Workshop on Structural Health Monitoring (EWSHM)*, Bilbao, Spain, 2016.

[49] A. R. Sagadeev, E. V. Vazhdaev, N. A. Avdonina, T. A. Zakurdaeva, and T. M. Levina, "Measurement of deformation of aircraft structures made of composite materials with fiber-optic sensors," in *In the the Proceedings of 2020 International Conference on Electrotechnical Complexes and Systems (ICOECS)*, Ufa, Russia, 2020, pp. 1—5.

[50] D. Zainal Abidin, S. Theminimulla, D. G. Waugh, and J. M. Griffin, "Optical fibers in composite materials: the effects on mechanical properties under flexural and tensile loading and acoustic emission monitoring the proceedings of the Institution of Mechanical Engineers, Part C," *J. Mech. Eng. Sci.*, vol. 236, no. 16, pp. 9169—9185, 2022.

[51] C. Schilder, M. Schukar, M. Steffen, and K. Krebber, "Structural Health monitoring of composite structures by distributed fibre optic sensors," in *In the Proceedings of the 5th International Symposium on NDT in Aerospace*, Singapore, 2013.

[52] B.-H. Choi and I.-B. Kwon, "Damage mapping using strain distribution of an optical fiber embedded in a composite cylinder after low-velocity impacts," *Composites, Part B*, vol. 173, p. 107009, 2019.

[53] M. Ciminello, S. Ameduri, B. Galasso, F. Romano, and A. Concilio, "Numerical and experimental comparison of impact damage detection by using distributed fiber optics on a stiffened composite panel," in *Dynamic Response and Failure of Composite Materials*, *Lecture Notes in Mechanical Engineering*, Springer, 2023, pp. 36—42.

[54] M. Nachtane, *et al*., "An overview of the recent advances in composite materials and artificial intelligence for hydrogen storage vessels design," *J. Compos. Sci.*, vol. 7, no. 3, p. 119, 2023.

[55] Y.-J. Lee, H. Ahmed, and J.-R. Lee, "Filament-wound composite pressure vessel inspection based on rotational through-transmission laser ultrasonic propagation imaging," *Compos. Struct.*, vol. 236, p. 111871, 2020.

[56] M. Froggatt and J. Moore, "High-spatial-resolution distributed strain measurement in optical fiber with Rayleigh scatter," *Appl. Opt.*, vol. 37, no. 10, pp. 1735—1740, 1998.

[57] E. Saeter, K. Lasn, F. Nony, and A. T. Echtermeyer, "Embedded optical fibres for monitoring pressurization and impact of filament wound cylinders," *Compos. Struct.*, vol. 210, pp. 608—617, 2019.

[58] R. Eisermann, *et al*., "Distributed strain sensing with sub-centimetre resolution for the characterisation of structural inhomogeneities and material degradation of industrial high-pressure composite cylinders," in *In the Proceedings of the 9th European Workshop on Structural Health Monitoring (EWSHM)*, Manchester, UK, 2018.

[59] M. Tomizuka, W. Blazejewski, A. Czulak, P. Gasior, J. Kaleta, and R. Mech, "SMART composite high pressure vessels with integrated optical fiber sensors," in *In the Proceedings of Sensors and Smart Structures Technologies for Civil, Mechanical, and Aerospace Systems*, 2010.

[60] A. Masoudi and T. P. Newson, "Contributed Review: distributed optical fibre dynamic strain sensing," *Rev. Sci. Instrum.*, vol. 87, no. 1, p. 011501, 2016.

[61] L. Palmieri, L. Schenato, M. Santagiustina, and A. Galtarossa, "Rayleigh-based distributed optical fiber sensing," *Sensors*, vol. 22, no. 18, p. 6811, 2022.

[62] R. Bernini, A. Minardo, and L. Zeni, "Dynamic strain measurement in optical fibers by stimulated Brillouin scattering," *Opt. Lett.*, vol. 34, no. 17, pp. 2613—2615, 2009.

[63] A. Voskoboinik, O. F. Yilmaz, A. W. Willner, and M. Tur, "Sweep-free distributed Brillouin time-domain analyzer (SF-BOTDA)," *Opt. Express*, vol. 19, no. 26, pp. B842—B847, 2011.

[64] A. Minardo, G. Porcaro, D. Giannetta, R. Bernini, and L. Zeni, "Real-time monitoring of railway traffic using slope-assisted Brillouin distributed sensors," *Appl. Opt.*, vol. 52, no. 16, pp. 3770—3776, 2013.

[65] White Paper, *Optical Backscatter Reflectometry (OBR) — Overview and Applications*, Roanoke, Virginia, USA, LUNA Innovations Inc, 2018. Available at: https://lunainc.com/sites/default/files/assets/files/resource-library/OBR-White-Paper-2018.09.12.pdf.

[66] D. Munzke, *et al*., "Distributed fiber-optic strain sensing with millimeter spatial resolution for the structural health monitoring of multiaxial loaded GFRP tube specimens," *Polym. Test.*, vol. 80, p. 106085, 2019.

[67] C. Schilder, M. Schukar, M. Steffen, and K. Krebber, "Evaluating distributed fibre optic sensors integrated into thermoplastic composites for structural health monitoring," in *In the Proceedings of the 23rd International Conference on Optical Fibre Sensors*, Santander, Spain, 2014, pp. 91575Q-91571—91575Q-91574.

[68] S. Loranger, M. Gagné, V. Lambin-Iezzi, and R. Kashyap, "Rayleigh scatter based order of magnitude increase in distributed temperature and strain sensing by simple UV exposure of optical fibre," *Sci. Rep.*, vol. 5, p. 11177, 2015.

[69] P. Sharma and S. Neogi, "Performance-based design and manufacturing of filament wound Type-4 cylinders for compressed gas storage," *Compos. Struct.*, vol. 309, p. 116710, 2023.

[70] H. Ahmadian, M. Yang, and S. Soghrati, "Effect of resin-rich zones on the failure response of carbon fiber reinforced polymers," *Int. J. Solids Struct.*, vols. 188—189, pp. 74—87, 2020.

[71] U. M. N. Jayawickrema, H. M. C. M. Herath, N. K. Hettiarachchi, H. P. Sooriyaarachchi, and J. A. Epaarachchi, "Fibre-optic sensor and deep learning-based structural health monitoring systems for civil structures: a review," *Measurement*, vol. 199, p. 111543, 2022.

[72] C. Karapanagiotis and K. Krebber, "Machine learning approaches in Brillouin distributed fiber optic sensors," *Sensors*, vol. 23, no. 13, p. 6187, 2023.

[73] D. F. Kandamali, X. Cao, M. Tian, Z. Jin, H. Dong, and K. Yu, "Machine learning methods for identification and classification of events in ϕ-OTDR systems: a review," *Appl. Opt.*, vol. 61, no. 11, pp. 2975—2997, 2022.

[74] S. Liehr, L. A. Jäger, C. Karapanagiotis, S. Münzenberger, and S. Kowarik, "Real-time dynamic strain sensing in optical fibers using artificial neural networks," *Opt. Express*, vol. 27, no. 5, pp. 7405—7425, 2019.

[75] A. Pedraza, D. del Río, V. Bautista-Juzgado, A. Fernández-López, and Á. Sanz-Andrés, "Study of the feasibility of decoupling temperature and strain from a ϕ-PA-OFDR over an SMF using neural networks," *Sensors*, vol. 23, no. 12, p. 5515, 2023.

[76] D.-P. Zhou, W. Li, L. Chen, and X. Bao, "Distributed temperature and strain discrimination with stimulated Brillouin scattering and Rayleigh backscatter in an optical fiber," *Sensors*, vol. 13, no. 2, pp. 1836—1845, 2013.

[77] X. Lu, M. A. Soto, and L. Thévenaz, "Temperature-strain discrimination in distributed optical fiber sensing using phase-sensitive optical time-domain reflectometry," *Opt. Express*, vol. 25, no. 14, pp. 16059—16071, 2017.

[78] M. N. Alahbabi, Y. T. Cho, and T. P. Newson, "Simultaneous temperature and strain measurement with combined spontaneous Raman and Brillouin scattering," *Opt. Lett.*, vol. 30, no. 11, pp. 1276—1278, 2005.

[79] X. Bao, D. J. Webb, and D. A. Jackson, "Combined distributed temperature and strain sensor based on Brillouin loss in an optical fiber," *Opt. Lett.*, vol. 19, no. 2, pp. 141—143, 1994.

[80] P. Stajanca, K. Hicke, and K. Krebber, "Distributed fiber optic sensor for simultaneous humidity and temperature monitoring based on polyimide-coated optical fibers," *Sensors*, vol. 19, no. 23, p. 5279, 2019.

[81] A. Charmi, S. Mustapha, B. Yilmaz, J. Heimann, and J. Prager, "A machine learning based-guided wave approach for damage detection and assessment in composite overwrapped pressure vessels," *ReJNDT*, vol. 1, no. 1, pp. 1—6, 2023.

[82] M. Saade and S. Mustapha, "Assessment of the structural conditions in steel pipeline under various operational conditions — a machine learning approach," *Measurement*, vol. 166, p. 108262, 2020.

[83] A. A. F. Ogaili, A. A. Jaber, and M. N. Hamzah, "A methodological approach for detecting multiple faults in wind turbine blades

based on vibration signals and machine learning," *Curved Layer. Struct.*, vol. 10, no. 1, p. 20220214, 2023.
[84] C. Hu and R. Albertani, "Machine learning applied to wind turbine blades impact detection," *Wind Eng.*, vol. 44, no. 3, pp. 325—338, 2019.
[85] L. Bornn, C. R. Farrar, and G. Park, "Damage detection in initially nonlinear systems," *Int. J. Eng. Sci.*, vol. 48, no. 10, pp. 909—920, 2010.
[86] H. Heidari Bafroui and A. Ohadi, "Application of wavelet energy and Shannon entropy for feature extraction in gearbox fault detection under varying speed conditions," *Neurocomputing*, vol. 133, pp. 437—445, 2014.
[87] B. Tang, W. Liu, and T. Song, "Wind turbine fault diagnosis based on Morlet wavelet transformation and Wigner-Ville distribution," *Renewable Energy*, vol. 35, no. 12, pp. 2862—2866, 2010.
[88] K. P. Murphy, *Machine Learning: A Probabilistic Perspective*, Cambridge, MA, USA, MIT Press, 2012.
[89] C. Karapanagiotis, K. Hicke, and K. Krebber, "Machine learning assisted BOFDA for simultaneous temperature and strain sensing in a standard optical fiber," *Opt. Express*, vol. 31, no. 3, pp. 5027—5041, 2023.

Bionotes

Christos Karapanagiotis
Bundesanstalt für Materialforschung und -prüfung (BAM), Unter den Eichen 87, 12205 Berlin, Germany
christos.karapanagiotis@bam.de
https://orcid.org/0000-0002-9065-3480

Christos Karapanagiotis received the Diploma in Physics from the Aristotle University of Thessaloniki, Greece, and his M.Sc. degree in Optics and Photonics from the Karlsruhe Institute of Technology (KIT), Germany, in 2018. Currently, he conducts research at the Federal Institute for Materials Research and Testing (BAM), Germany, and his research interests include distributed fiber optic sensors and machine learning in non-destructive testing (NDT) applications. Publication list: https://orcid.org/0000-0002-9065-3480.

Marcus Schukar
Bundesanstalt für Materialforschung und -prüfung (BAM), Unter den Eichen 87, 12205 Berlin, Germany

Marcus Schukar received his graduate engineer degree at the University of Applied Sciences FHTW, Berlin, Germany, in 2006. Currently, he is engaged as an engineer at the BAM Federal Institute for Materials Research and Testing (BAM), Germany, where he is involved in the research and development of fiber optic sensors for a variety of applications, including distributed fiber optic sensors for structural health monitoring of composite structures. A comprehensive bibliography can be obtained from the BAM Publication Server PUBLICA (https://www.bam.de/Navigation/EN/News/Publications/publications.html).

Katerina Krebber
8.6 Faseroptische Sensorik, Bundesanstalt fur Materialforschung und -prufung, Berlin, Germany

Dr. Katerina Krebber studied physics and received the PhD degree in electrical engineering. She has more than 20 years experience with the development of fibre optic sensors. Since 2004 she has been with BAM. At BAM she is head of the Division Fibre Optic Sensors and leader of a number of R&D projects. She is an author and a co-author of more than 200 scientific publications. A comprehensive bibliography can be obtained from the BAM Publication Server PUBLICA (https://www.bam.de/Navigation/EN/News/Publications/publications.html).